Phase shifter calibration in phase-shifting interferometry

Yeou-Yen Cheng and James C. Wyant

This paper describes some practical methods to calibrate the phase shifter in phase-shifting interferometry (PSI). The phase shifter used in the experiment is a piezoelectric transducer (PZT) that has a nonlinearity of <l%. Using the quantitative method described in this paper, the repeatability in the measurement of the phase-shifting angle is ˜9.046° rms, and the 3σ value is 0.139°. A calibration-insensitive phase calculation algorithm is discussed and compared with other synchronous detection equations (e.g., the three-bucket or the four-bucket method). Experimental results verify the calibration-insensitive mechanism of the self-calibrating algorithm.

I. Introduction

The high measurement accuracy of the electronic phase-measurement techniques makes phase-shifting interferometry (PSI)[1-3] very useful for interferometric optical testing. Well-known advantages of the PSI include (1) high measurement accuracy, (2) rapid measurement, (3) good results even with low contrast fringes, (4) results independent of intensity variations across the pupil, (5) phase obtained at a fixed grid of data points, and (6) the polarity of the wave front can be determined. The basic idea of PSI is that, if the phase difference between the two interfering beams is made to vary in some known manner such as changing in discrete steps (stepping) or changing linearly with time (ramping), three or more measurements of the intensity distribution across the pupil for different phase shifts between the interfering beams can be used to determine the phase distribution across the pupil. The most common way to vary the phase difference between the two interfering beams is to mount the reference mirror on a piezoelectric transducer (PZT) and change the voltage to the PZT. In practice, it is easier to take the data while the phase difference varies linearly with time rather than in discrete steps; if discrete steps are used, a sufficient delay must exist between changing the phase and taking data for any transients to damp out.

The calibration of the PZT for proper phase shift between data frames is a very important issue if good phase measurement results are to be obtained using PSI.[3] Although this paper focuses on the discussion of methods for PZT calibration, it may be applied to other techniques to introduce phase shifts. Two fundamental problems associated with the motion of the PZT-driven reference mirror are unknown sensitivity of the PZT, where the reference mirror may not move to the right position to introduce an expected amount of phase shift (e.g., 90°) unless a careful calibration has been done first, and nonlinearity of the PZT (since the equations used for phase calculations are based on an assumption that the PZT is linear in its motion, this problem can introduce a considerable error if the nonlinearity is large). Both problems will generate a kind of sinusoidal phase error that has twice the spatial frequency of the interference fringes if conventional synchronous detection equations are used to calculate the phase of the wave front under test. Figure 1 illustrates a typical result where the phase shift between frames is supposed to be 90° but is actually 88°.

Two commonly used methods to move the PZT are stepping and ramping. Stepping involves moving the reference mirror in several discrete steps and then taking and storing the intensity readings in the computer before the mirror moves to the next position. Ramping means to move the reference mirror at a rate linearly with time. The computer reads the intensity readings out of the integrating detector array as the reference mirror moves. Each detector pixel will integrate the intensity over a time interval that depends on the number of integrating buckets used for the phase calculation. For the four-bucket method, the time interval of integration is selected so the phase changes by $\pi/2$ during one integration interval.

Two methods proposed earlier for PZT calibration are the "phase-lock" method and the "sinusoidal extrema sensing" method as described by Koliopoulos.[2] The phase-lock method has the advantage that pre-

The authors are with University of Arizona, Optical Sciences Center, Tucson, Arizona 85721.

Received 25 February 1985.
0003-6935/85/183049-04$02.00/0.
© 1985 Optical Society of America

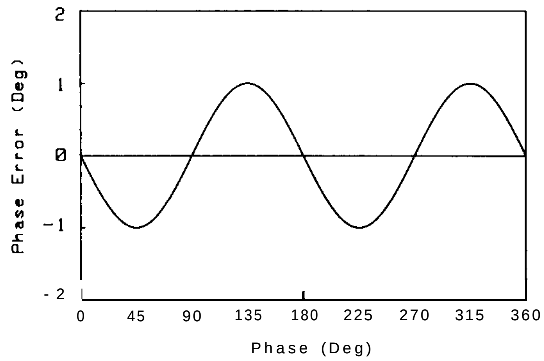

Fig. 1. Phase error vs phase for a phase step of 88° rather than 90°.

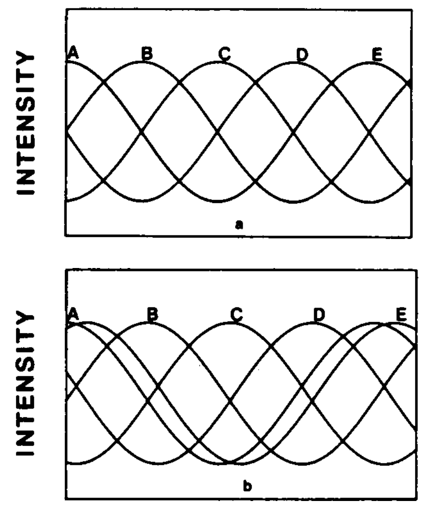

Fig. 2. Display of five frames of phase-shifted fringe patterns for PZT calibration: (a) β = 90°, (b) β = 96°.

calibration of the PZT, either for incorrect sensitivity or nonlinearity, is not required. But this method requires extra electronics (e.g., a nonintegrating detector) and the phase-stepping angle must be 90° rather than another value. Also, this method can be used for phase stepping only.

The extrema sensing method is precalibration work that occurs before any phase measurement. It uses the integrating detector array itself to monitor the intensity variations over a phase interval a little larger than 2π while the PZT is ramping. Then the intensity variation function on any pixel can be used to convolve with a bipolar function to find the zero crossing positions (phase = n π). To locate positions where the phase is equal to $(2n + 1)\pi/2$, another discrete convolution is needed to get the second derivative. Because of the discrete nature of the convolution, a linear interpolation is also needed to get the true zero crossing position. Since the PZT may not move uniformly across the pupil, many points across the pupil must be monitored to characterize the PZT. This requires more time, and greater error caused by air turbulence may occur.

Another alternative of the extrema sensing technique is storing and displaying four sets of 1 - D intensity profiles across the array for different phase shifts. The extrema position can then be located either visually or by using differentiating techniques. If the phase shifts are 90°, the first and the third or the second and the fourth intensity profiles should be 180° out of phase. To get a higher accuracy of the PZT calibration, a differentiating technique is needed. If the mirror surface is not good enough, high frequency structure on the intensity profile will make the differentiating technique troublesome and confusing. In this paper some practical ways to perform PZT calibrations are described. These methods usually give better results for ramping the PZT rather than stepping it.

II. Linear PZT

When the nonlinearity of the PZT is zero, one can average two sets of measured phase data that were calculated from two sets of intensity readings that are 90° offset with respect to each other. For example, by using successive $\pi/2$ phase shifts, four sets of intensity readings, ***A, B, C,*** and ***D,*** can be obtained. Using the "three measurement of four-bucket" algorithm," *A*, *B*, and C can generate one set of phase data while B, C, and D can generate another set. Since the sinusoidal calibration error has spatial frequency twice that of the fringe pattern, the error can be canceled by simply averaging these two sets of phase data. Of course, the completeness of the cancellation depends on how close the offset phase angle is to 90°. Furthermore, unless the nonlinearity is zero, the cancellation will not be 100%.

III. Small Nonlinearity of the PZT

In general, even good quality PZTs have a small amount of nonlinearity ranging from <l% to a few percent. Since these PZTs also have some hysteresis and thermal drift that make the small amount of nonlinearity not repeatable, it is difficult to calibrate this small and nonrepeatable nonlinearity. Some practical ways to do the PZT calibration (assuming that the nonlinearity of the PZT is small enough that the equations for phase calculation still work) follow.

A. Display Five Intensity Frames

The simplest method to provide an estimate, within ±3°, of the phase shift is to display five phase-shifted intensity profiles of tilt fringes simultaneously on the screen of the monitor. If the PZT is calibrated well enough that the phase shifts are exactly 90°, the last intensity profile will coincide with the first and the eye cannot see any offset between the two as known in Fig. 2(a). But when phase increments are not 90°, the last profile will deviate from the first and can be detected visually. If the offset is about a quarter of the phase increment, the phase-shifting angle is ˜90° ± 6°. Figure 2(b) shows the five intensity profiles when the phase-shifting angle is equal to 96°. An accuracy of ±3° is possible by simply adjusting the knob on the PZT driver and making the offset as small as possible.

B. Use Equations to Calculate the Phase-Shifting Angle

Equation (1) can be used to calculate the phase-shifting angle at each pixel to obtain a more accurate value. From Eq. (l), which is the equation of the intensity distribution of an interferogram, four unknowns (including the phase-shifting angle β) can be found:

$$I(x,y) = I_0\{1 + \gamma \cos[\phi(x,y) + \beta]\}. \qquad (1)$$

Thus, one needs at least four intensity readings to solve for β. As mentioned in Ref. 3, if the phase shifts are arranged as 0, β,3β, and 4β, then β can be solved easily. Since we are ramping the PZT and have five buckets (A, B, C, D, and E), if the first two and last two buckets are used we should be able to calculate β in the same way. The required four buckets are

$$A(x,y) = \int_{-2.5\beta}^{-1.5\beta} I_0\{1 + \gamma \cos[\phi(x,y) + \psi(t)]\}d\psi(t), \qquad (2)$$

$$B(x,y) = \int_{-1.5\beta}^{-0.5\beta} I_0\{1 + \gamma \cos[\phi(x,y) + \psi(t)]\}d\psi(t), \qquad (3)$$

$$D(x,y) = \int_{+0.5\beta}^{+1.5\beta} I_0\{1 + \gamma \cos[\phi(x,y) + \psi(t)]\}d\psi(t), \qquad (4)$$

$$E(x,y) = \int_{+1.5\beta}^{+2.5\beta} I_0\{1 + \gamma \cos[\phi(x,y) + \psi(t)]\}d\psi(t). \qquad (5)$$

Rewriting them we have

$$A(x,y) = I_0'\left(1 + \gamma \left\{\cos\phi \left[\sin\left(\frac{5\beta}{2}\right) - \sin\left(\frac{3\beta}{2}\right)\right] + \sin\phi \left[\cos\left(\frac{3\beta}{2}\right) - \cos\left(\frac{5\beta}{2}\right)\right]\right\}\right), \qquad (6)$$

$$B(x,y) = I_0'\left(1 + \gamma \left\{\cos\phi \left[\sin\left(\frac{3\beta}{2}\right) - \sin\left(\frac{\beta}{2}\right)\right] + \sin\phi \left(\frac{\beta}{2}\right) - \cos\left(\frac{3\beta}{2}\right)\right]\right\}\right), \qquad (7)$$

$$D(x,y) = I_0'\left(1 + \gamma \left\{\cos\phi \left[\sin\left(\frac{3\beta}{2}\right) - \sin\left(\frac{\beta}{2}\right)\right] + \sin\phi \left[\cos\left(\frac{3\beta}{2}\right) - \cos\left(\frac{\beta}{2}\right)\right]\right\}\right), \qquad (8)$$

$$E(x,y) = I_0'\left(1 + \gamma \left\{\cos\phi \left[\sin\left(\frac{5\beta}{2}\right) - \sin\left(\frac{3\beta}{2}\right) + \sin\phi \left[\cos\left(\frac{5\beta}{2}\right) - \cos\left(\frac{3\beta}{2}\right)\right]\right\}\right). \qquad (9)$$

From Eqs. (6) through (9), β can be solved as

$$\beta = \cos^{-1}\left[\left(\frac{1}{2}\right)\left(\frac{A - E}{B - D}\right)\right]. \qquad (10)$$

Note, when A - E and B - D are very small, the uncertainty of β becomes larger. If the PZT has some amount of nonlinearity, it behaves like a singular point. This problem can be solved by putting several tilt fringes across the array and averaging all the calculated values of β. This method is much more accurate than the previous one because it provides numerical results. By measuring β a hundred times, the standard deviation is ~0.046° and the 3σ value is ~0.139°.

C. PZT Calibration-Insensitive Algorithm

Since the accuracy of the phase value calculated from the conventional phase-calculation algorithms (e.g., three-bucket or four-bucket) is quite sensitive to PZT calibration as shown in Fig. 3, the PZT must be precalibrated to ensure there is no drift from the required phase-shifting angle. Also, most PZTs have some nonuniformity in their motion such that some tilt will be introduced and nonuniform phase shift will be present across the pupil. Of course, a higher quality PZT driver provides three independent gain controls to compensate for the nonuniformity; but it is best if an algorithm intrinsically insensitive to PZT calibration is obtained. The key point is to make sure that the equation for phase calculations contains a phase-shifting angle term to automatically compensate for variations of phase-shifting angle β. Next, the derivation of the equation of the PZT calibration insensitive algorithm for ramping is given. If the phase-shifting angle is β and the phase starts shifting at –2β, the four integrated buckets look like

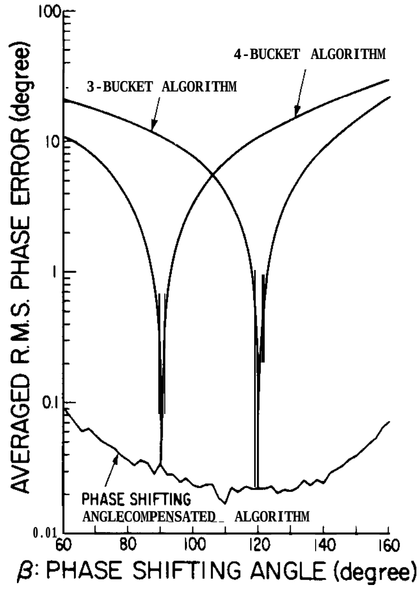

Fig. 3. Averaged rms phase error vs different phase-shifting angles β for three different phase calculation algorithms.

$$A(x,y) = \int_{-2\beta}^{-\beta} \{I_1 + I_2 \cos[\phi(x,y) + \psi(t)]\}d\psi(t), \qquad (11)$$

$$B(x,y) = \int_{-\beta}^{0} \{I_1 + I_2 \cos[\phi(x,y) + \psi(t)]\}d\psi(t), \qquad (12)$$

$$C(x,y) = \int_{0}^{+\beta} \{I_1 + I_2 \cos[\phi(x,y) + \psi(t)]\}d\psi(t), \qquad (13)$$

$$D(x,y) = \int_{+\beta}^{+2\beta} \{I_1 + I_2 \cos[\phi(x,y) + \psi(t)]\}d\psi(t). \qquad (14)$$

Rewriting these equations we have

$$A(x,y) = I_1' + I_2\{\cos\phi[\sin(2\beta) - \sin\beta] + \sin\phi[\cos\beta - \cos(2\beta)]\}, \qquad (15)$$

$$B(x,y) = I_1' + I_2[\cos\phi \sin\beta + \sin\phi(1 - \cos\beta)], \qquad (16)$$

$$C(x,y) = I_1' + I_2[\cos\phi \sin\beta + \sin\phi(\cos\beta - 1)], \qquad (17)$$

$$D(x,y) = I_1' + I_2\{\cos\phi[\sin(2\beta) - \sin\beta] + \sin\phi[\cos(2\beta) - \cos\beta]\}. \qquad (18)$$

Let

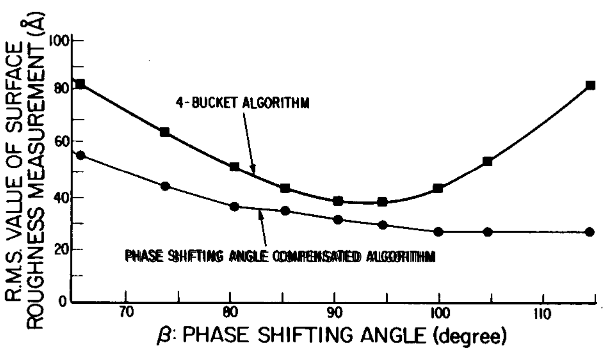

Fig. 4. Surface roughness measurement vs different phase-shifting angle β for both the four-bucket algorithm and the phase-shifting angle compensated algorithm.

$$U = B - C, \quad M = T - W,$$
$$V = A - D, \quad N = 3U - V,$$
$$W = A + D, \quad P = U + V,$$
$$T = B + C, \quad Q = V - U.$$

From Eqs. (15) through (18) one has

$$\beta = \cos^{-1}\left(\frac{Q}{2U}\right), \tag{19}$$

or

$$\beta = \tan^{-1}\left(\frac{\sqrt{NP}}{Q}\right). \tag{20}$$

Although Eq. (20) can be used to calculate β, the results are worse than that of the four measurement of five-bucket method mentioned earlier. The phase value can be obtained from Eqs. (15) through (18) and given by

$$\phi(x,y) = \tan^{-1}\left[\left(\frac{Q}{M}\right)\tan\beta\right]. \tag{21}$$

Note that in Eq. (21) the factor (tan β) is included in the phase calculation, thus it can automatically compensate any deviation of phase-shifting angle β caused by bad calibration or nonuniform motion of the PZT. Rewriting Eq. (21) we have

$$\phi(x,y) = \tan^{-1}\left(\frac{\sqrt{NP}}{M}\right), \tag{22}$$

or

$$\phi(x,y) = \tan^{-1}\left[\frac{\sqrt{[(B - C) + (A - D)][3(B - C) - (A - D)]}}{(B + C) - (A + D)}\right]. \tag{23}$$

This result is the same as that shown in Carré's papers in 1966, although he derived it for the phase stepping method and phase shifts of 4πα. The quadrant for ϕ is determined by checking the sign of U and M as defined above. Figure 3 shows a computer simulation result for averaged phase error (in rms) vs different phase-shifting angles for three different phase calculation algorithms. Both three-bucket (120° phase shift) and four-bucket (90° phase shift) algorithms are quite sensitive to calibration error, but the phase-shifting angle compensated algorithm is not sensitive to this kind of error over a wide range of β. It is interesting to note that, for the calibration-insensitive algorithms, the averaged phase error is minimum for β = 110° (and not 90° as might be expected). This result is quite close to Carré's prediction.[5] Some experimental results are shown in Fig. 4 to verify the theoretical predictions. Six or seven tilt fringes are sampled by the linear detector array; the rms values of the surface roughnesses are compared for the four-bucket algorithm and the calibration-insensitive algorithm for different values of β. If the dc bias term, which is caused by surface roughness, is subtracted out, the effect of the PZT calibration error is obviously worse for the four-bucket algorithm; but for the calibration-insensitive algorithm the result is quite repeatable for the variation of β from 80° to 115°.

IV. Conclusions

In conclusion, the phase measurement error is sensitive to calibration error if conventional synchronous detection equations of PSI are used to do the phase calculations. By displaying five phase-shifted tilt fringe patterns, the phase shifting can be determined with an accuracy of ±3°. The numerical method discussed in this paper can provide a better repeatability with a standard deviation of ~0.046° and the 3σ value is ~0.139°. If the calibration-insensitive algorithm is used, the averaged phase error is quite small (<λ/3600) as the phase-shifting angle changes from 60° to 160° as shown in Fig. 3. Another advantage of this algorithm is that the problem of pupil-dependent shifter sensitivity is eliminated. One disadvantage of the algorithm is that a longer calculation time is needed because of the complexity of the phase calculation equation.

References

1. J. H. Bruning, "Fringe Scanning Interferometers," in Optical *Shop Testing,* D. Malacara, Ed. (Wiley, New York, 1978).
2. C. Koliopoulos, "Interferometric Optical Phase Measurement Techniques," Ph.D. Dissertation, Optical Sciences Center, U. Arizona (1981).
3. J. Schwider, R. Burow, K. E. Elssner, J. Grzanna, R. Spolaczyk, and K. Merkel, "Digital Wave-Front Measuring Interferometry: Some Systematic Error Sources," Appl. Opt. 22,342l (1983).
4. J. B. Hayes, "Linear Methods of Computer Controlled Optical Figuring," Ph.D. Dissertation, Optical Sciences Center, U. Arizona (1984).
5. P. Carré "Installation et utilisation du comparateur photoelectrique et interferentiel du Bureau International des Poids et Mesures," Metrologia 2,13 (1966).